JACC: BASIC TO TRANSLATIONAL SCIENCE VOL. 4, NO. 2, 2019

PRECLINICAL RESEARCH

Glucagon Receptor Antagonism Ameliorates Progression of Heart Failure

Chen Gao, PhD,[a] Shuxun Vincent Ren, MD, PhD,[a] Junyi Yu, MD,[a,b] Ulysis Baal,[a] Dung Thai, MD, PhD,[c,d] John Lu, MD, PhD,[c,d] Chunyu Zeng, MD, PhD,[b] Hai Yan, PhD,[c,d] Yibin Wang, PhD[a]

VISUAL ABSTRACT

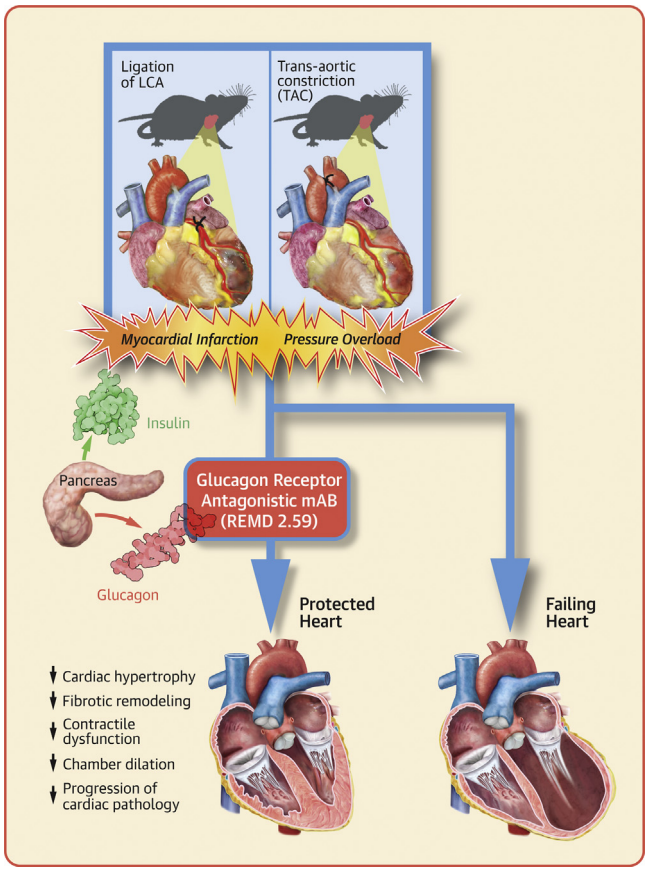

Gao, C. et al. J Am Coll Cardiol Basic Trans Science. 2019;4(2):161–72.

HIGHLIGHTS

- **Systemic treatment of an antibody-based glucagon receptor antagonist confers cardioprotection against myocardial infarction and post-myocardial infarction remodeling in mice.**
- **Systemic treatment of glucagon receptor antagonist prevents pressure overload induced cardiac remodeling and dysfunction in mice.**
- **Glucagon receptor antagonist treatment attenuates the pathological progression of heart failure induced by pressure overload in mice.**
- **Long-term suppression of glucagon signaling is potentially an effective therapy for heart failure with different etiologies independent of metabolic disorders.**

From the [a]Department of Anesthesiology, Cardiovascular Research Laboratories, David Geffen School of Medicine, University of California, Los Angeles, Los Angeles, California; [b]Department of Cardiology, Daping Hospital, The Third Military Medical University, Chongqing, China; [c]REMD Biotherapeutics, Camarillo, California; and [d]Beijing Cosci-REMD Biotherapeutics, Beijing, China. This work is supported in part by National Institutes of Health grants HL140116 to Dr. Wang. Dr. Gao is a recipient of Postdoctoral Fellowship from American Heart Association (17POST33661136). Drs. Thai, Lu, and Yan are employees of REMD Biotherapeutics. Dr. Wang has served as consultant for REMD Biotherapeutics. All other authors have reported that they have no relationships relevant to the contents of this paper to disclose.

ISSN 2452-302X https://doi.org/10.1016/j.jacbts.2018.11.001

JACC: BASIC TO TRANSLATIONAL SCIENCE VOL. 4, NO. 2, 2019
APRIL 2019:161–72

ABBREVIATIONS AND ACRONYMS

GCGR = glucagon receptor

GLC = glucagon

MI = myocardial infarction

PBS = phosphate-buffered saline

PCR = polymerase chain reaction

TAC = transaortic constriction

SUMMARY

Mice were treated with a fully human monoclonal glucagon receptor antagonistic antibody REMD2.59 following myocardial infarction or pressure overload. REMD2.59 treatment blunted cardiac hypertrophy and fibrotic remodeling, and attenuated contractile dysfunction at 4 weeks after myocardial infarction. In addition, REMD2.59 treatment at the onset of pressure overload significantly suppressed cardiac hypertrophy and chamber dilation with marked preservation of cardiac systolic and diastolic function. Initiation of REMD2.59 treatment 2 weeks after pressure overload significantly blunted the progression of cardiac pathology. These results provide the first in vivo proof-of-concept evidence that glucagon receptor antagonism is a potentially efficacious therapy to ameliorate both onset and progression of heart failure. (J Am Coll Cardiol Basic Trans Science 2019;4:161–72)

Heart failure affects approximately 6.5 million people over 20 years of age in the United States, with its prevalence estimated to increase about 45% by 2030 to almost 8 million (1). It is a chronic disease with complex etiology and heterogeneity in its pathological manifestations. Major risk factors for heart failure include smoking, hypertension, and obesity, as well as lifestyle and dietary influences. Despite significant advancement in the standard care of heart failure, the 5-year mortality rate of the disease remains at nearly 50% (1). The new effective therapies for heart failure are critically needed for such a major unmet need.

SEE PAGE 173

Glucagon (GLC) is a peptide hormone produced by pancreatic α-cells (2–6). As a major catabolic hormone, GLC stimulates glucose production from glycogen in liver and promotes gluconeogenesis while it inhibits glycolysis and glycogen synthesis (4). It increases blood glucose and energy expenditure as part of the energy mobilization process in response to hypoglycemia and other bioenergetic stress. Consequently, GLC serves as a counterbalancing hormone with insulin to regulate glucose homeostasis depending on nutrient conditions and available energy sources (7). The GLC receptor (GCGR) is a member of the G protein-coupled receptor family (3,6,8,9). The canonical function of GCGR elicited by GLC is mediated by G protein-coupled protein kinase A activation; however, tissue-specific function of GCGR has been implicated in different cellular processes (2,3,10). Elevated GLC is observed in chronic hyperglycemia associated with type 1 or type 2 diabetes (11–13). Overactivated GLC signaling may contribute to disease progression of diabetes by enhancing glucose production and aggravating systemic hyperglycemia, as well as impairing insulin signaling. Therefore, GCGR inhibition, using either small molecules or antagonistic antibodies, is potentially efficacious to treat diabetes as demonstrated in both preclinical studies as well as several recent clinical trials (11–21). However, much of the previous studies on GLC signaling are in the liver and brain, involving glucose metabolic regulation (2,3,22). Its specific and cell-autonomous role in cardiac tissue has just begun to be appreciated.

Other than glucose regulation in liver, GCGR is also widely expressed in multiple other tissues, including the heart (3,15,18,23–28). In a recent study by Ali et al. (29), GLC stimulation was shown to promote ischemia injury in mouse heart while cardiomyocyte specific GCGR inactivation protected the heart from pathological remodeling following myocardial infarction. This study highlights the potential cardiomyocyte cell-autonomous effect of GCGR overactivation in cardiac pathological remodeling, and GCGR antagonism as a potential therapy for heart failure. REMD-477 is a fully human anti-GCGR antibody that competitively blocks GLC binding to the GCGR with 30-pM binding affinity, and can effectively inhibit the receptor activity at low nanomolar concentrations in cell-based functional assays (14,17,20). Compared with small-molecule approaches (30), antibody-based GCGR antagonism such as REMD-477 is a competitive antagonist and does not have deleterious effects on serum lipid profiles (11,12,19,21,31). Finally, REMD-477

All authors attest they are in compliance with human studies committees and animal welfare regulations of the authors' institutions and Food and Drug Administration guidelines, including patient consent where appropriate. For more information, visit the *JACC: Basic to Translational Science* author instructions page.

Manuscript received April 2, 2018; revised manuscript received November 1, 2018, accepted November 2, 2018.

has been shown to be safe in a phase I study (NCT02715193) and is being tested in 2 phase II clinical studies (NCT03117998 and NCT02455011 for type 1 and type 2 diabetes, respectively). In short, anti-GCGR antibody offers a novel tool to effectively and specifically inhibit GCGR with proven record of clinical safety and efficacy at molecular and metabolic levels.

Functionally identical as REMD-477, REMD2.59 is a surrogate human antibody specifically generated for preclinical studies in rodents (32). In a recent study, weekly treatment with REMD2.59 is shown to reverse diabetes in *ob/ob* mice and improves cardiac function associated with diabetic cardiomyopathy (32). Although this study supports the cardioprotective effect of GCGR antagonism, it is not clear whether the beneficial effect is a direct consequence of cardioprotection on cardiomyocyte or an indirect result of improved global glucose homeostasis and insulin signaling. In the current study, we employed 2 mechanistically divergent and diabetes-independent murine disease models for heart failure, myocardial infarction, and pressure overload, to test whether the cardioprotection by the GCGR antibody is the primary effect of the receptor inhibition. Based on morphological, functional, and molecular parameters, treatment with GCGR antibody REMD2.59 significantly ameliorated the development of heart failure, by attenuating pathological remodeling and cardiac hypertrophy while preventing functional deterioration and pathological gene expression. These novel and exciting observations implicate a potential role of GLC-mediated signaling in heart failure via a cardiomyocyte cell-autonomous mechanism. It raises the prospect of targeting GCGR as potential therapy to treat common forms of heart failure independent of the confounding status of global glucose metabolic disorders.

METHODS

ANIMALS. C57BL/6 male mice (Jackson Laboratory, Bar Harbor, Maine) were used in this study, and all mice were housed in groups of 4 to 5 mice per cage in a room maintained at 23 ± 1°C and 55 ± 5% humidity with a 12-h light-dark cycle and given ad libitum access to food and water.

MYOCARDIAL INFARCTION. Myocardial infarction (MI) was induced in mice by ligation of the left anterior coronary artery. Briefly, the chest was opened via a left thoracotomy. The left coronary artery was identified visually using a stereo microscope, and a 7-0 suture (Ethicon, Inc., Somerville, New Jersey) was placed around the artery 1 to 2 mm below the left auricle. The electrocardiogram was monitored continuously. Permanent occlusion of the left coronary artery resulted from its ligation with the suture. Myocardial ischemia was confirmed by pallor in heart color and ST-segment elevation. The chest was closed with 6-0 silk suture. Once spontaneous respiration resumed, the endotracheal tube was removed.

TRANSAORTIC CONSTRICTION. In the transaortic constriction (TAC) study, after intubation using a 20-gauge plastic needle, mice were placed on a volume ventilator (80 breaths/min, 1.2 ml/g/min) and the anesthesia maintained by isoflurane. The chest was opened via a limited incision in the third intercostal space. The aorta was identified at the T8 region. A 6-0 silk suture was passed around the transverse aorta and tightened against a 27-gauge needle followed by the removal of the needle. Pressure gradient was evaluated by transaortic Doppler.

TREATMENT PROTOCOL. For the MI study, a total of 56 C57BL/6 male mice 8 to 10 weeks of age were operated on by occluding the left anterior coronary artery. Then they were randomly divided into 3 groups: 1) vehicle-treated (phosphate-buffered saline [PBS]) control mice (n = 20); 2) monoclonal antibody against GCGR-treated (mAb REMD2.59) mice (n = 18; 7 mg/kg, subcutaneously, 2 injections at 2 h and 14 days post-MI); and 3) GLC-treated mice (n = 18; 30 μg/kg body weight in 10% gelatin, 4 times/day for the first 6 days). For the TAC study, C57BL6 mice at 6 to 7 weeks of age were randomly divided into 2 groups: 5 sham operated as baseline control mice and 29 mice operated for TAC. The TAC-operated animals were randomly divided into 3 treatment groups: 1) vehicle treated (n = 11; antibody dilation buffer A: 10-mM NaAcetate, 5% sorbitol, 0.004% Tween 20, pH 5.2, weekly subcutaneous injection); 2) REMD2.59 treated (n = 7; 7 mg/kg, subcutaneous injection, weekly started at the onset of TAC); and 3) REMD2.59 therapy (n = 11; 7 mg/kg, subcutaneous injection, weekly started 2 weeks after the onset of TAC).

CARDIAC PHYSIOLOGY. For echocardiography, in vivo cardiac function was assessed by transthoracic echocardiography (Acuson P300, 18-MHz transducer, Siemens [Siemens Healthcare Diagnostics, Tarrytown, New York] and VisualSonics 2100 [Fujifilm Visualsonics, Toronto, Ontario, Canada]) in conscious mice for the MI study and anesthetized mice for the TAC study. From left ventricle short-axis view, an M-mode echocardiogram was acquired to measure left ventricular end-systolic and diastolic diameters. Ejection fraction and fractional shortening were calculated using onboard software package (Vevo Imaging System 2100 [Fujifilm Visualsonics]).

Imaging acquisition and analyses were performed by investigators blinded to treatments. For hemodynamic measurements, a Mikro-tip catheter (SPR1000, Millar Instruments, Houston, Texas) was inserted into the left ventricle. Left ventricular pressure was recorded with the Powerlab Data Acquisition System (ADInstruments Inc., Colorado Springs, Colorado) and calculated into left ventricular developed pressure as end-systolic pressure minus end-diastolic pressure, as well as positive maximal left ventricular pressure derivative (+dp/dtmax) and negative maximal left ventricular pressure derivative (−dp/dtmax) using Chart 7 software (AD Instruments, Colorado Springs, Colorado).

HISTOLOGICAL STUDIES. Hearts were fixed with 10% buffered formalin, embedded in paraffin, and sectioned at 4 μm. One middle longitudinal section per heart was stained with Masson's trichrome (HT-15, Sigma-Aldrich, St. Louis, Missouri). Eight randomly selected fields (400×) from the noninfarct area in the left ventricle were examined for fibrosis and myocyte size under a microscope. Each group comprised 5 to 6 hearts, and a minimum of 40 fields were analyzed in each group by computerized planimetry (ImageJ, National Institutes of Health, Bethesda, Maryland). To assess fibrosis, fibrotic blue area and whole myocardial area were measured. The fibrotic area was presented as a percentage of fibrotic area to the myocardial area. Myocyte size was measured in cross-sectioned muscle cells. In total, 100 to 150 cells/heart were analyzed based on wheat germ agglutinin staining. Two methods were used to assess the size of the infarcted heart. Infarct area was calculated as a percentage of infarcted ventricular area to total ventricular area using the front and back sides of the heart photos. Infarct size was measured as a percentage of infarcted ventricular wall length to total ventricular wall length using cardiac sections. The observer was blinded to the origin of the cardiac sections.

TUNEL assay was performed with the In-Situ Apoptosis Detection Kit (Thermo Fisher Scientific, Waltham, Massachusetts). Briefly, hearts were fixed by perfusion with 10% formalin solution, embedded in paraffin, and sectioned at 6 μm. One middle longitudinal section per heart was taken for TUNEL staining. Proteinase K (20 μg/ml) was added to each slide. Endogenous peroxidases were inactivated by covering sections with 2% hydrogen peroxide. After fixation, sections were incubated with terminal deoxynucleotidyl transferase buffer at 37°C for 30 min. Reactions were terminated with 1× saline-sodium citrate buffer. After being washed, slides were incubated with RTU streptavidin-horseradish peroxidase for 30 min. Positive signal was developed by adding DAB solution. After counterstained with RTU hematoxylin, slides were covered by mounting medium and analyzed under a microscope. Each group comprised 5 to 6 hearts. Eight fields (400×) from the infarct area per heart were analyzed for positive cells and total cells using computerized planimetry (ImageJ). The degree of apoptosis was presented as a percentage of positive cells to total cells.

TABLE 1 Reverse-Transcription-Polymerase Chain Reaction Primer Oligonucleotides

Primer Name	Sequence
BNP RT-F	TAGCCAGTCTCCAGAGCAATTC
BNP RT-R	TTGGTCCTTCAAGAGCTGTCTC
18s F	TCAAGAACGAAAGTCGGAGG
18s R	GGACATCTAAGGGCATCAC

REAL-TIME POLYMERASE CHAIN REACTION. 1 μg RNA was used for first-strand complementary DNA synthesis using Random Primer (Thermo Fisher Scientific) and SuperScriptII Reverse Transcriptase (Thermo Fisher Scientific) according to manufacturer's instruction. Real-time polymerase chain reaction (PCR) was performed using IQ SYBR Green Supermix (Bio-Rad Laboratories, Hercules, California) with CFX-96 Real-time PCR Detection System (Bio-Rad Laboratories) with primers as described in Table 1.

STATISTICAL ANALYSIS METHODS. We used student Wilcoxon rank sum test or analysis of variance to perform statistical analysis between 2 groups or among multiple groups, and a p value <0.05 was considered significant. The specific p values are depicted in the figures according to the following symbols, unless specified in individual figure legend: # indicates $p < 0.05$, * indicates $p < 0.01$, ** indicates $p < 0.001$.

RESULTS

GCGR ANTAGONISM ATTENUATES MI-INDUCED CARDIAC REMODELING. Eight-week to 10-week-old C57BL/J6 male mice were operated by permanent occlusion of left coronary artery descending artery and then randomized into 3 experimental groups, which were treated with PBS (control group; subcutaneous injection twice at 2 h, and 14 days post-MI) or monoclonal anti-GCGR antibody REMD2.59 (REMD group; subcutaneous injection of 7 mg/kg twice at 2 h and 14 days post MI) and GLC (GLC group; subcutaneous injection of 30 μg/kg 4 times/day for the first 6 days), as

illustrated in Figure 1A. REMD2.59 treatment modestly but significantly reduced fasting blood glucose level, indicating the expected GLC antagonistic effect of REMD2.59 in mice (Figure 1B). As shown in Figures 2A and 2B, in the vehicle-treated control group, histopathology analysis at the end of the experiment period of 4 weeks post-MI showed approximately 39% infarct scar size relative to total heart size. In contrast, the REMD-treated heart showed an average of 32% scar area and GLC-treated hearts showed an average of 48% scar area. Although GLC-treated hearts trended to have larger infarct sizes and REMD-treated hearts trended to smaller infarct sizes, the differences did not reach statistical significance, indicating that myocardium sparing may not be the major basis of protection GCGR effects in the post-MI hearts. The REMD2.59-treated heart showed a significant reduction in the apoptotic events detected by TUNEL (Figures 2C and 2D) as well as the level of myocardial fibrosis measured by trichrome staining (Figures 2E and 2F). However, the cellular identities of the apoptotic cells remain to be determined. Finally, REMD2.59 treatment also significantly reduced cardiac hypertrophy versus the vehicle-treated group based on heart weight (Figure 3A), or myocyte cross-sectional area measurements (Figure 3B). However, treatment of unoperated mice with REMD2.59 for 2 weeks did not affect basal heart weight (Figure 3C). These data support the notion that GCGR antagonism can prevent and attenuate the onset of pathological remodeling in response to myocardial injury, by reducing fibrosis and attenuating cardiomyocyte pathological hypertrophy.

GCGR ANTAGONISM PRESERVES CARDIAC FUNCTION AFTER MI. In addition to morphological and histological analysis, we measured cardiac function in each experimental group by both noninvasive echocardiogram and catheter based hemodynamic analysis. As shown in Figures 4A and 4B, a serial echocardiogram showed progressive deterioration of systolic function from 26% fractional shortening at week 1 to 16% at week 4 after MI in the vehicle-treated mice. In contrast, the REMD2.59 treatment almost completely preserved cardiac function from 30% fractional shortening at week 1 to 38% at week 4. In contrast, the mice treated with GLC showed earlier contractile dysfunction than the vehicle-treated group, losing fractional shortening from 26% at week 1 to 17.9% at week 1 after MI. Consistent with the impact on systolic function, significant chamber dilation was observed in the vehicle- and GLC-treated groups, which was almost completely blunted by REMD2.59 treatment (Figure 4B). Using catheter-based invasive hemodynamic measurements (Figures 4C–E), we observed that REMD2.59 treatment significantly elevated left ventricular developed pressure, and systolic pressure and improved both systolic (+dP/dtmax; $p < 0.05$) and diastolic (-dP/dtmax; $p = 0.06$) parameters in the post-MI hearts compared with the vehicle-treated control mice. These data suggest that GCGR inhibition can prevent loss of cardiac function in post-MI hearts. It is noted that the mice from hemodynamic studies had average heart rates (378 ± 94 beats/min, 363 ± 71 beats/min, 431 ± 114 beats/min for vehicle-, REMD-, and GLC-treated groups, respectively). In contrast, the average heart rates of mice for the echocardiograph studies were 626 ± 18 beats/min, 657 ± 9 beats/min, and 662 ± 7 beats/min for the same groups, respectively. Therefore, the hemodynamic measurements were measured under a significantly depressed state, likely due to anesthesia. Nevertheless, there were no differences in heart rates among the 3 experiment groups in either measurements, suggesting that the differences observed in the hemodynamic or echocardiographic parameters were not the results of differential degrees of anesthesia levels.

GCGR INHIBITION ON PRESSURE OVERLOAD–INDUCED CARDIAC HYPERTROPHY. To demonstrate the applicability of GCGR antagonism therapy to heart failure with different etiologies, we investigated the impact of REMD2.59 on pressure overload induced cardiac hypertrophy, dysfunction, and remodeling. Pressure overload was induced by TAC as described previously (33,34) in C57BL/6 male mice 8 to 10 weeks of age

FIGURE 1 Glucagon and Glucagon Receptor Antagonism in Myocardial Infarction

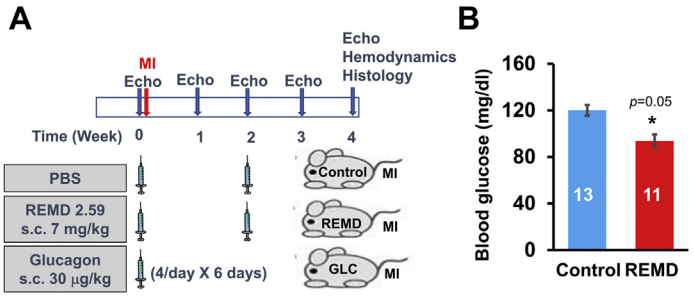

(A) Illustration of experimental design to investigate the effect of glucagon (GLC) and REMD2.59 treatment on myocardial infarction (MI). **(B)** Blood glucose level 14 days after vehicle (Control) or REMD treatment as indicated. The statistical significance and the specific p values depicted in this and the following figures are described in the Methods section according to the following symbols, unless specified for specific comparison among specific groups: #$p < 0.05$, *$p < 0.01$, **$p < 0.001$. Echo = echocardiography; PBS = phosphate-buffered saline; s.c. = subcutaneous.

FIGURE 2 Impact of GLC and GLC Receptor Antagonism on Myocardial Infarction

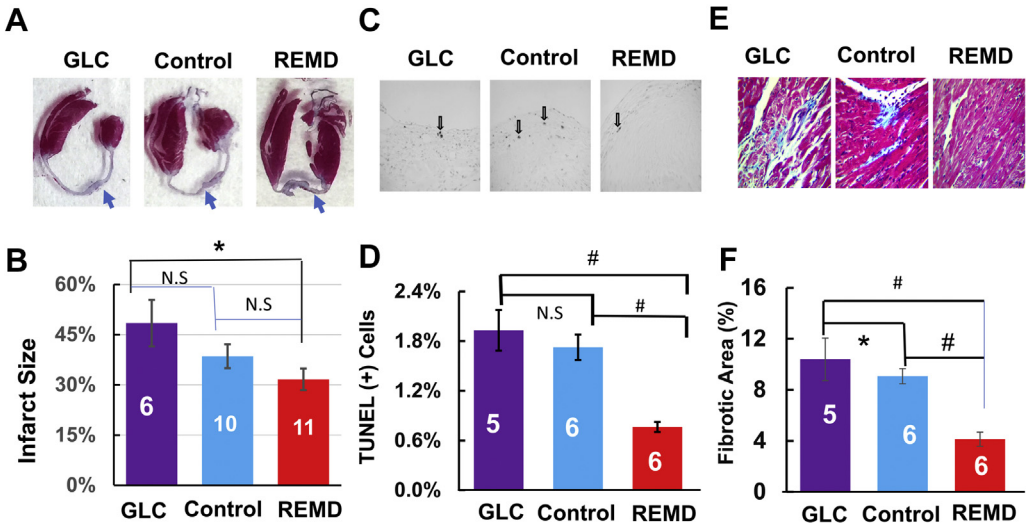

(A) Representative hematoxylin and eosin section of cardiac tissue 4 weeks after MI treated with PBS (Control), GLC, and GLC receptor antagonist (REMD). **(B)** Quantification of infarct scar sizes based on histological analysis; group sizes are indicated in each bar graph. **(C)** Representative TUNEL staining images of left ventricle with apoptotic cells indicated by **arrows**. **(D)** Quantification of percent TUNEL-positive cells with group sizes indicated. #$p < 0.01$. **(E)** Representative trichrome staining of left ventricular tissue. **(F)** Quantification of fibrotic area in the noninfarcted left ventricle from each group with group sizes indicated. Abbreviations as in Figure 1.

FIGURE 3 Impact of GLC and GLC Receptor Antagonist on Cardiac Hypertrophy in Post-Myocardial Infarct Heart

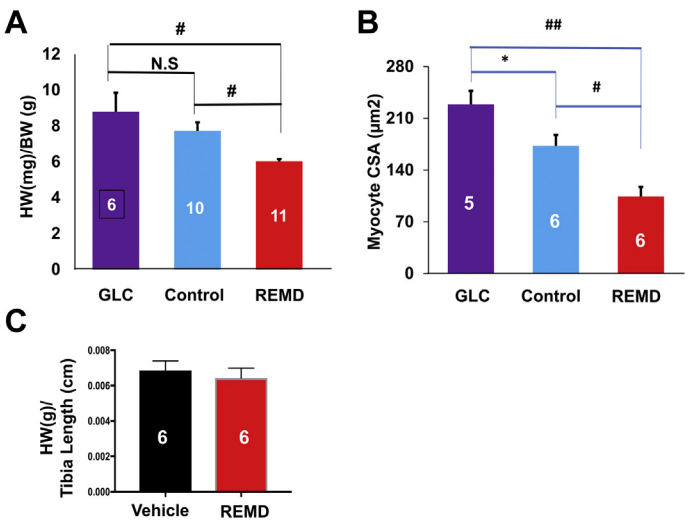

(A) Heart weight (HW) versus body weight (BW) 4 weeks after MI treated with PBS (Control), GLC, and GLC receptor antagonist (REMD). Groups sizes are indicated. **(B)** Myocyte cross-sectional areas (CSA) in left ventricles of the same mouse groups as in pane **A**. Group sizes are indicated. ## $p < 0.001$, #$p < 0.01$, *$p < 0.05$. Abbreviations as in Figure 1.

followed by weekly treatment of vehicle or anti-GCGR antibody (REMD2.59, 7 mg/kg body weight, subcutaneous injection) starting at the same time or starting at 2-weeks post TAC (REMD2.59 therapy) (Figure 5). Compared with the sham-operated group, TAC induced a significant increase in heart sizes as demonstrated in histological sections of the left ventricle, and tissue weights and cardiomyocyte cross-sectional morphometric data of cardiac chamber weight and the left ventricle (Figure 6). Concurrent treatment with REMD2.59 significantly blunted the increase of heart weight and myocyte enlargement compared with the TAC group. In contrast, starting REMD2.59 treatment at 2 weeks post-TAC (REMD2.59 therapy) failed to block left ventricular hypertrophy. These data indicate that GCGR inhibition can prevent the onset of cardiac hypertrophy induced by pressure overload, but has limited effect to reverse established cardiac hypertrophy.

GCGR INHIBITION IN PRESSURE OVERLOAD–INDUCED CARDIAC DYSFUNCTION. Using serial echocardiogram analysis, we found cardiac function, as measured from ejection fraction and percent fractional shortening, was significantly impaired by chronic pressure overload as early as 2 weeks post-TAC and deteriorated further at 5 weeks post-TAC (Figure 7),

FIGURE 4 Impact of GLC and GLC Receptor Antagonist on Cardiac Function and Chamber Dilation in Post-Myocardial Heart

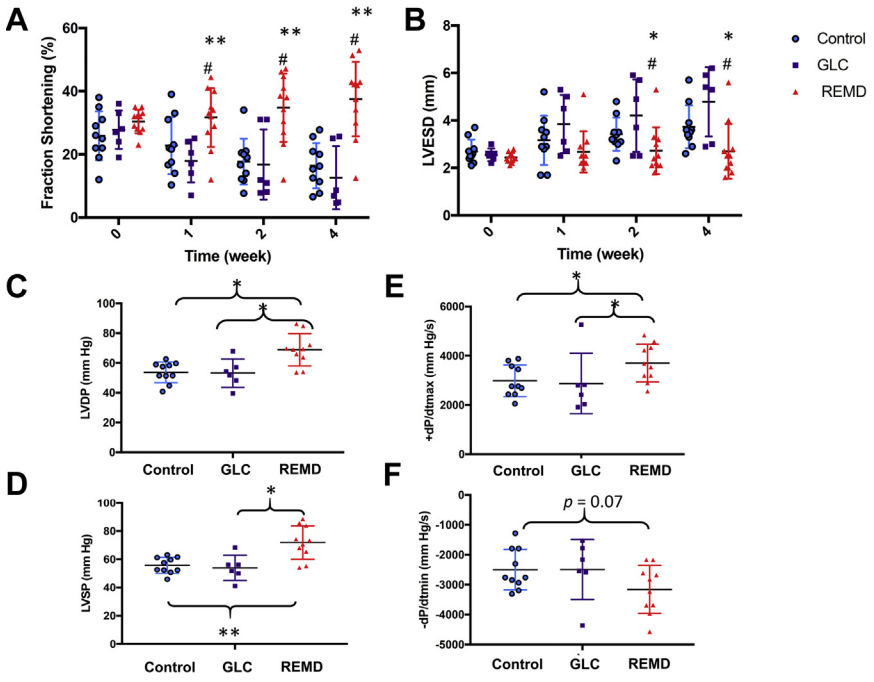

(A) Fractional shortening and **(B)** left ventricular end-systolic dimension (LVESD) in MI hearts treated with PBS (Control; n = 10, **blue**), GLC (n = 6, **purple**), and GLC receptor antagonist (REMD; n = 11; **red**) at different time points recorded by echocardiogram. #p < 0.05 REMD versus Control; REMD versus GLC. **(C)** Left ventricular developed pressure (LVDP). **(D)** Left ventricular systolic pressure (LVSP). **(E)** Maximum pressure derivative (+dP/dtmax) and **(F)** Minimum pressure derivative (-dP/dtmin) as measured by conductance catheter. Abbreviations as in Figure 1.

along with pulmonary congestion (Figure 6B). Treating mice with REMD2.59 at the onset of pressure overload largely preserved the contractile function in the pressure-overloaded hearts with ejection fraction and percent fractional shortening statistically unchanged comparing with the sham-operated mice at 5 weeks post-TAC (Figure 7). Starting REMD2.59 treatment 2 weeks after TAC, when functional impairment had already manifested, blunted further deterioration comparing to the vehicle-treated group. Using speckle tracking-based tissue-strain analysis from echocardiographic images (Figure 8), we observed that REMD2.59 treatment from the onset of TAC prevented the pressure overload-induced systolic and diastolic dysfunction as demonstrated in both systolic strain and diastolic strain rate. In contrast, REMD2.59 treatment starting 2 weeks post-TAC had limited success to reverse these parameters. The cardioprotective effect of REMD2.59 treatment was also manifested in significantly blunted pulmonary congestion (Figure 6B). All these evidences suggest that GCGR antagonism exerts significant protection against pressure overload induced cardiac dysfunction and blunts progression of heart failure.

GCGR ANTAGONISM ON PATHOLOGICAL REMODELING IN THE PRESSURE-OVERLOADED HEART. As a common feature of cardiac remodeling, chronic

FIGURE 5 Glucagon and Glucagon Antagonism in Pressure-Overload Induced Cardiac Hypertrophy

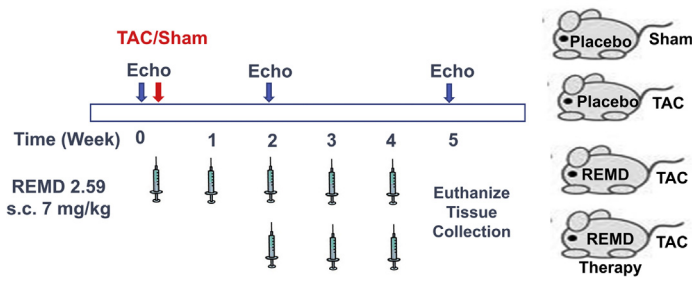

Illustration of treatment regiments for pressure overload-induced heart failure by GLC receptor antagonist either at the onset of the transaortic surgery (transaortic constriction [TAC] + REMD) or 2 weeks after (TAC + REMD therapy). Abbreviations as in Figure 1.

FIGURE 6 Impact of GLC Receptor Antagonist on Cardiac Hypertrophy

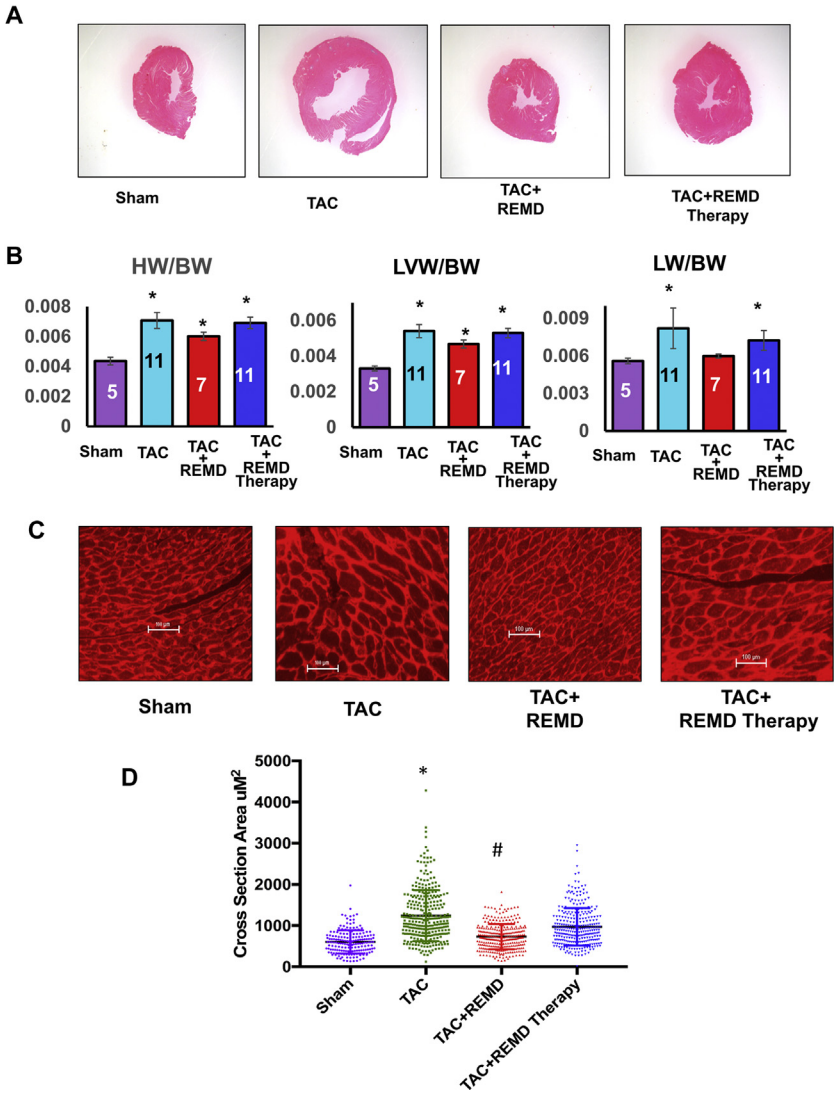

(A) Representative histological section of ventricle by hematoxylin and eosin staining of the heart from each treatment group as indicated. **(B)** Tissue weight measured at week 5 post-TAC from each treatment group as indicated, including HW versus BW (HW/BW), left ventricle weight versus BW (LVW/BW), and lung weight versus BW (LW/BW). *$p < 0.05$ versus sham. **(C)** Representative images of tissue section of left ventricles stained with wheat germ agglutinin from each treatment group as indicated. **(D)** Quantification of cardiomyocyte cross-sectional area in left ventricles of hearts from different treatment groups as indicated. *$p < 0.05$ versus Control, #$p < 0.05$ versus TAC. Abbreviations as in Figures 1, 3, and 5.

pressure overload induced significant level of cardiac fibrosis, as detected by trichrome staining (Figures 9A and 9B) and the expression of a pathological marker gene B-type natriuretic peptide measured by quantitative reverse transcription PCR (Figure 9C). REMD2.59 treatment started either at the onset of pressure overload or 2 weeks post-TAC completely blocked these changes. Therefore, GCGR inhibition can significantly block pathological remodeling in stressed heart in terms of extracellular matrix remodeling or gene expression.

DISCUSSION

In this report, the therapeutic effect of a GCGR antagonistic antibody REMD2.59 was tested in 2 mechanistically divergent disease models of heart failure without confounding defects in global

FIGURE 7 **Functional Impact of GLC Receptor Antagonist on Contractile Function Measured by Echocardiogram**

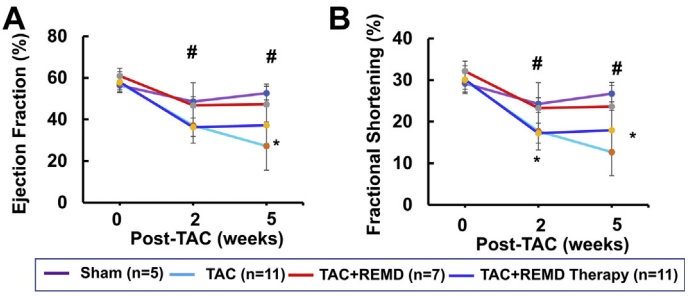

(A) Ejection fraction and **(B)** fractional shortening were measured at basal (week 0), 2 weeks post-TAC (week 2) and 5 weeks post-TAC from each treatment group as indicated. *p < 0.05 TAC versus TAC + REMD; #p < 0.05 TAC versus TAC + REMD therapy. Abbreviations as in Figures 1 and 5.

FIGURE 8 **Impact of GLC Receptor Antagonist on Pressure-Overloaded Heart Measured by Tissue Strain**

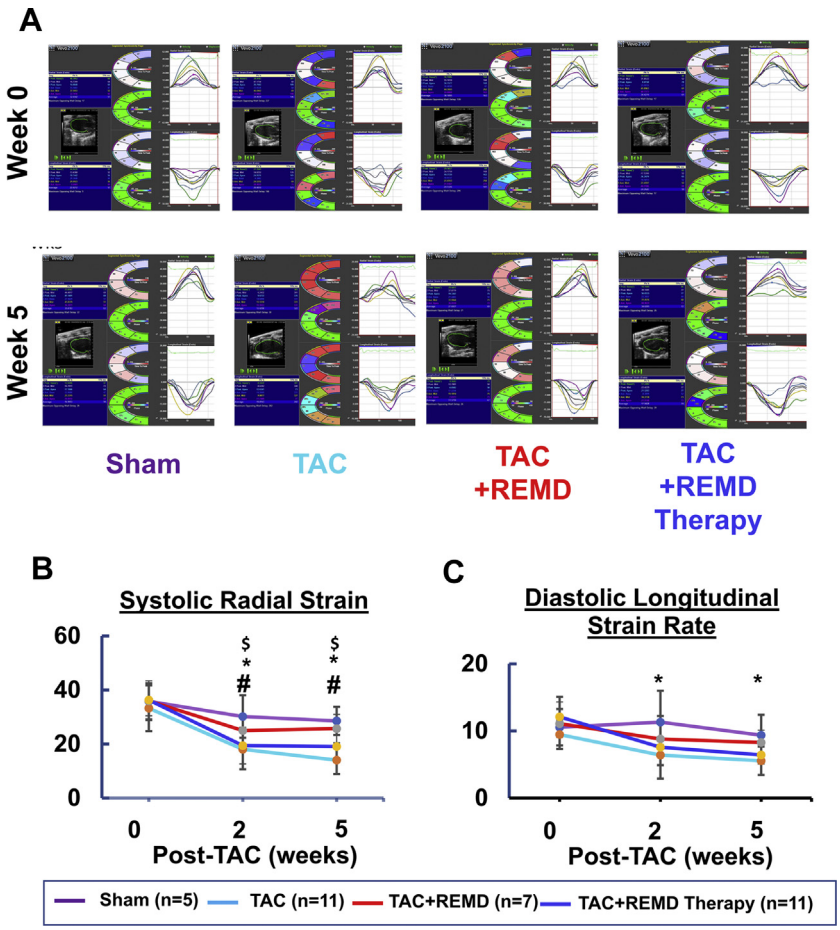

(A) Representative images of long-axis echo recording **(left panel)**, with cross-sectional segment synchronicity map **(middle panels)**, and radial and longitudinal endocardial strain **(right panel)**. **(B)** Average systolic radial strain and **(C)** average diastolic longitudinal strain rates at week 0, 2, and 5 post-TAC from each experimental group as indicated. *p < 0.05 Control versus TAC; #p < 0.05 TAC versus TAC+REMD; $p < 0.05 Control versus TAC + REMD therapy. Abbreviations as in Figures 1 and 5.

FIGURE 9 Impact of GLC Receptor Antagonist on Pathological Remodeling

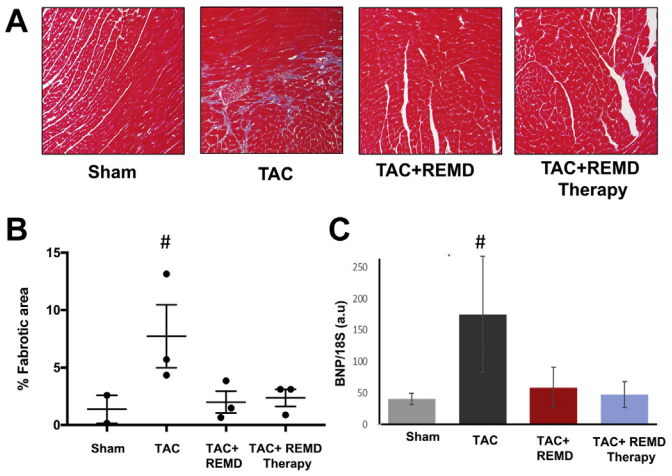

(A) Representative images of trichrome-stained tissue section from hearts of different experimental groups as indicated. **(B)** Quantification of cardiac fibrosis from panel **A**. **(C)** messenger RNA expression level of B-type natriuretic peptide as measured by quantitative reverse transcriptase polymerase chain reaction in heart tissue from different experimental groups as indicated. n = 3/group. #$p < 0.05$ versus Sham. Abbreviations as in Figures 1 and 5.

metabolism. Based on histological and functional analyses in both MI-injured and pressure-overloaded hearts, REMD2.59 treatment showed significant protection against cardiac hypertrophy and fibrosis remodeling with better preserved contractile function. These findings support a broadly applicable cardioprotective effect of GCGR inhibition against heart failure with different etiologies. As both these pathological stressors are imposed specifically and directly on heart rather in a systemic fashion, the observed cardioprotection of REMD2.59 is likely the result of its direct impact on GCGR signaling in cardiomyocytes rather than its impact on global glucose metabolic activities. This observation is consistent with the previous observations made in the cardiomyocyte-specific GCGR knockout mice, which have demonstrated the cardioprotective effect of GCGR antagonism against myocardial infarction in a receptor-dependent and cardiomyocyte cell-autonomous manner (29,32).

GLC and insulin are both pancreatic but counterbalancing hormones important to maintain systemic glucose regulation. GLC exerts its function via a peptide G protein-coupled receptor, GCGR. The canonical GCGR-mediated signaling involves classic G protein-coupled cAMP-dependent protein kinase A activation in hepatocytes, leading to induction of gluconeogenesis and glycogen catabolism, while inhibiting glycolysis (7,35). In addition to its predominant expression in liver, GCGR is also expressed at modest to low levels in the kidney, heart, pancreas, and many other tissues (3,8,36). Although G protein-coupled canonical signaling for GLC is well established in hepatocytes, other mechanisms involving intracellular calcium regulation have also been reported in nonhepatocytes including cardiomyocytes (3,10,28,36). In this report, we investigated GCGR inhibition in 2 mechanistically divergent disease models (i.e., myocardial infarction vs. pressure overload), the treatment resulted in similar cardioprotective effects against a broad spectrum of sequential pathological features in the failing heart, including cardiomyocyte hypertrophy, marker gene induction, interstitial fibrosis, and most importantly, cardiomyocyte contractile dysfunction. Apparently, GCGR antagonism is affecting cellular processes shared by different etiologies of cardiac pathology, including diabetes (32), ischemic injury, and mechanical overload. It is conceivable that abnormal GCGR activity may impact on cellular metabolism and energetic status via AMPK-dependent modulation in working heart as shown by Sharma et al. (32). However, our understanding to noncanonical signaling mechanism of GCGR is still very limited, and more studies are needed to illustrate the mechanistic basis of GCGR antagonism-mediated cardioprotection in response to different pathological stressors and energy homeostasis in failing hearts.

It is important to note that when REMD2.59 was applied 2 weeks after the onset of pressure overload,

GCGR antagonism no longer had any significant impact on cardiac hypertrophy, but still preserved the residual functions of the heart (**Figures 6 and 7**). This is consistent with previously reported observation that cardiomyocyte hypertrophy is established rather early in response to pressure overload while contractile dysfunction and fibrotic remodeling will continue to manifest (33). Our results highlight the potential limitation in the therapeutic window for heart failure. Nevertheless, REMD treatment can halt the further progression of heart failure and remodeling despite the limitation that GCGR antagonism may not be sufficient to reverse established cardiac hypertrophy and to fully restore contractile function. It is clear that more studies will be needed to fully establish the therapeutic efficacy of GCGR antagonism. Clinically relevant large animal models with established heart failure will be needed, and longer-term treatment and better outcome-based measurements (e.g., death and exercise tolerance) will be required.

Extensive pharmacological and structural analysis shows GCGR antibody REMD-477 competitively blocks GLC binding to the GCGR with 30-pM binding affinity, and can fully inhibit the receptor activity at low nanomolar concentrations in cells (14,17,20). Functionally identical to REMD-477, REMD2.59 is a surrogate human antibody specifically generated for chronical preclinical studies in rodents and primates. Unlike previous small-molecule approaches (30), REMD-477 does not have deleterious effects on serum lipid profiles (11,12,19,21,31) in both ongoing clinical trials in diabetes patients. In short, the anti-GCGR antibody as tested here offers a novel and powerful therapeutic tool to effectively and specifically inhibit GCGR with proven record of clinical safety and efficacy at molecular and metabolic levels.

Several other diabetic therapies, including GLC-like peptide-1 agonists (37,38), dipeptidyl peptidase 4 inhibition (39), and sodium glucose cotransporter 2 inhibitors (40,41), have demonstrated various degrees of cardiovascular benefits along with ameliorated metabolic defects in glucose homeostasis. Yet, not all glucose-lowering therapies have such significant cardiovascular protective effects as sodium glucose cotransporter 2 inhibition (42–46). It is also unclear if these therapies will be efficacious for common forms of heart failure without the confounding metabolic disorders. Our current study in 2 heart failure disease models free from systemic metabolic disorders further supports that GCGR inhibition may be repurposed as an effective therapy for common forms of heart failure.

ACKNOWLEDGMENT The authors wish to thank Ms. Haiying Pu for excellent technical assistance.

ADDRESS FOR CORRESPONDENCE: Dr. Yibin Wang or Dr. Chen Gao, Department of Anesthesiology, Cardiovascular Research Laboratories, David Geffen School of Medicine, University of California, Los Angeles, 650 Charles E. Young Drive, Room CHS 37-200J, Los Angeles, California 90095. E-mail: yibinwang@mednet.ucla.edu OR gaochen0813@g.ucla.edu.

PERSPECTIVES

COMPETENCY IN MEDICAL KNOWLEDGE: Systemic treatment of an antibody-based GCGR antagonist is currently in phase I and II clinical trials for type 1 and type 2 diabetes. The current study demonstrates for the first time that systemic treatment of GCGR antagonist can also exert potent cardioprotection against ischemic injury in the heart, and prevents pathological remodeling and heart failure induced by mechanic overload in nonobese and nondiabetic mice.

TRANSLATIONAL OUTLOOK: Systemic treatment of GCGR antagonist can be considered as a potential therapy for heart failure with different etiologies without concurrent metabolic disorders.

REFERENCES

1. Benjamin EJ, Blaha MJ, Chiuve SE, et al. Heart Disease and Stroke Statistics-2017 Update: a report From the American Heart Association. Circulation 2017;135:e146–603.

2. Vuguin PM, Charron MJ. Novel insight into glucagon receptor action: lessons from knockout and transgenic mouse models. Diabetes Obes Metab 2011;13 Suppl 1:144–50.

3. Authier F, Desbuquois B. Glucagon receptors. Cell Mol Life Sci 2008;65:1880–99.

4. Jiang G, Zhang BB. Glucagon and regulation of glucose metabolism. American journal of physiology Endocrinol Metab 2003;284:E671–8.

5. Nakamura S, Rodbell M. Glucagon induces disaggregation of polymer-like structures of the alpha subunit of the stimulatory G protein in liver membranes. Proc Natl Acad Sci U S A 1991;88:7150–4.

6. Levey GS, Weiss SR, Ruiz E. Characterization of the glucagon receptor in a pheochromocytoma. J Clin Endocrinol Metab 1975;40:720–3.

7. Holst JJ, Holland W, Gromada J, et al. Insulin and glucagon: partners for life. Endocrinology 2017;158:696–701.

8. Yamato E, Ikegami H, Takekawa K, et al. Tissue-specific and glucose-dependent expression of receptor genes for glucagon and glucagon-like peptide-1 (GLP-1). Horm Metab Res 1997;29:56–9.

9. MacNeil DJ, Occi JL, Hey PJ, Strader CD, Graziano MP. Cloning and expression of a human

glucagon receptor. Biochem Biophys Res Commun 1994;198:328–34.

10. Xu Y, Xie X. Glucagon receptor mediates calcium signaling by coupling to G alpha q/11 and G alpha i/o in HEK293 cells. J Recept Sig Transduct Res 2009;29:318–25.

11. Bagger JI, Knop FK, Holst JJ, Vilsboll T. Glucagon antagonism as a potential therapeutic target in type 2 diabetes. Diabetes Obes Metab 2011;13:965–71.

12. Gu W, Yan H, Winters KA, et al. Long-term inhibition of the glucagon receptor with a monoclonal antibody in mice causes sustained improvement in glycemic control, with reversible alpha-cell hyperplasia and hyperglucagonemia. J Pharmacol Exp Ther 2009;331:871–81.

13. Ali S, Drucker DJ. Benefits and limitations of reducing glucagon action for the treatment of type 2 diabetes. Am J Physiol Endocrinol Metab 2009;296:E415–21.

14. Pettus J, Reeds D, Santos Cavaiola T, et al. Effect of a glucagon receptor antibody (REMD-477) in type 1 diabetes: a randomized controlled trial. Diabetes Obes Metab 2018;20:1302–5.

15. Dean ED, Li M, Prasad N, et al. Interrupted glucagon signaling reveals hepatic alpha cell axis and role for L-glutamine in alpha cell proliferation. Cell Metab 2017;25:1362–73.e5.

16. Yang DH, Zhou CH, Liu Q, Wang MW. Landmark studies on the glucagon subfamily of GPCRs: from small molecule modulators to a crystal structure. Acta Pharmacol Sin 2015;36:1033–42.

17. Wang MY, Yan H, Shi Z, et al. Glucagon receptor antibody completely suppresses type 1 diabetes phenotype without insulin by disrupting a novel diabetogenic pathway. Proc Natl Acad Sci U S A 2015;112:2503–8.

18. Lefebvre PJ, Paquot N, Scheen AJ. Inhibiting or antagonizing glucagon: making progress in diabetes care. Diabetes Obes Metab 2015;17:720–5.

19. Mu J, Qureshi SA, Brady EJ, et al. Anti-diabetic efficacy and impact on amino acid metabolism of GRA1, a novel small-molecule glucagon receptor antagonist. PLoS One 2012;7:e49572.

20. Yan H, Gu W, Yang J, et al. Fully human monoclonal antibodies antagonizing the glucagon receptor improve glucose homeostasis in mice and monkeys. J Pharmacol Exp Ther 2009;329:102–11.

21. Lau YY, Ma P, Gibiansky L, et al. Pharmacokinetic and pharmacodynamic modeling of a monoclonal antibody antagonist of glucagon receptor in male ob/ob mice. AAPS J 2009;11:700–9.

22. Hollenstein K, de Graaf C, Bortolato A, Wang MW, Marshall FH, Stevens RC. Insights into the structure of class B GPCRs. Trends Pharmacol Sci 2014;35:12–22.

23. Pujadas G, Drucker DJ. Vascular biology of glucagon receptor superfamily peptides: mechanistic and clinical relevance. Endocr Rev 2016;37:554–83.

24. Zhang H, Qiao A, Yang D, et al. Structure of the full-length glucagon class B G-protein-coupled receptor. Nature 2017;546:259–64.

25. Li Y, Sun J, Li D, Lin J. Activation and conformational dynamics of a class B G-protein-coupled glucagon receptor. Phys Chem Chem Phys 2016;18:12642–50.

26. Yang L, Yang D, de Graaf C, et al. Conformational states of the full-length glucagon receptor. Nat Commun 2015;6:7859.

27. Charron MJ, Vuguin PM. Lack of glucagon receptor signaling and its implications beyond glucose homeostasis. J Endocrinol 2015;224:R123–30.

28. Siu FY, He M, de Graaf C, et al. Structure of the human glucagon class B G-protein-coupled receptor. Nature 2013;499:444–9.

29. Ali S, Ussher JR, Baggio LL, et al. Cardiomyocyte glucagon receptor signaling modulates outcomes in mice with experimental myocardial infarction. Mol Metab 2015;4:132–43.

30. Filipski KJ, Bian J, Ebner DC, et al. A novel series of glucagon receptor antagonists with reduced molecular weight and lipophilicity. Bioorg Med Chem Lett 2012;22:415–20.

31. Gu W, Lloyd DJ, Chinookswong N, et al. Pharmacological targeting of glucagon and glucagon-like peptide 1 receptors has different effects on energy state and glucose homeostasis in diet-induced obese mice. J Pharmacol Exp Ther 2011;338:70–81.

32. Sharma AX, Quittner-Strom EB, Lee Y, et al. Glucagon receptor antagonism improves glucose metabolism and cardiac function by promoting AMP-mediated protein kinase in diabetic mice. Cell Rep 2018;22:1760–73.

33. Gao C, Ren S, Lee JH, et al. RBFox1-mediated RNA splicing regulates cardiac hypertrophy and heart failure. J Clin Invest 2016;126:195–206.

34. Lee JH, Gao C, Peng G, et al. Analysis of transcriptome complexity through RNA sequencing in normal and failing murine hearts. Circ Res 2011;109:1332–41.

35. Wu F, Song G, de Graaf C, Stevens RC. Structure and function of peptide-binding G protein-coupled receptors. J Mol Biol 2017;429:2726–45.

36. Rodgers RL. Glucagon and cyclic AMP: time to turn the page? Curr Diabetes Rev 2012;8:362–81.

37. Drucker DJ. The cardiovascular biology of glucagon-like peptide-1. Cell Metab 2016;24:15–30.

38. Seferovic PM, Petrie MC, Filippatos GS, et al. Type 2 diabetes mellitus and heart failure: a position statement from the Heart Failure Association of the European Society of Cardiology. Eur J Heart Fail 2018;20:853–72.

39. Nauck MA, Meier JJ, Cavender MA, Abd El Aziz M, Drucker DJ. Cardiovascular actions and clinical outcomes with glucagon-like peptide-1 receptor agonists and dipeptidyl peptidase-4 inhibitors. Circulation 2017;136:849–70.

40. Tanaka H, Hirata KI. Potential impact of SGLT2 inhibitors on left ventricular diastolic function in patients with diabetes mellitus. Heart Fail Rev 2018;23:439–44.

41. Kaplan A, Abidi E, El-Yazbi A, Eid A, Booz GW, Zouein FA. Direct cardiovascular impact of SGLT2 inhibitors: mechanisms and effects. Heart Fail Rev 2018;23:419–37.

42. Packer M. Worsening heart failure during the use of DPP-4 inhibitors: pathophysiological mechanisms, clinical risks, and potential influence of concomitant antidiabetic medications. J Am Coll Cardiol HF 2018;6:445–51.

43. Packer M. Contrasting effects on the risk of macrovascular and microvascular events associated with anti-hyperglycaemic drugs that enhance sodium excretion and lower blood pressure. Diabet Med 2018;35:707–13.

44. Lim S, Eckel RH, Koh KK. Clinical implications of current cardiovascular outcome trials with sodium glucose cotransporter-2 (SGLT2) inhibitors. Atherosclerosis 2018;272:33–40.

45. Bistola V, Lambadiari V, Dimitriadis G, et al. Possible mechanisms of direct cardiovascular impact of GLP-1 agonists and DPP4 inhibitors. Heart Fail Rev 2018;23:377–88.

46. Nassif M, Kosiborod M. Effect of glucose-lowering therapies on heart failure. Nat Rev Cardiol 2018;15:282–91.

KEY WORDS glucagon receptor antagonism, heart failure, myocardial infarction, pressure overload